# Supplementary material

## Theoretical considerations

Stern-Volmer quenching constant ($K_{sv}$) and quenching rate constant ($k_q$) were calculated using **Equation S1**:

$$\frac{F_0}{F} = 1 + k_q\tau_0[Q] = 1 + K_{sv}[Q] \quad \textbf{(Equation S1)}$$

where $F_0$ = initial tryptophan fluorescence intensity of HSA, $F$ = tryptophan fluorescence intensity of HSA after the addition of a quencher, $k_q$ = quenching rate constants of the biomolecule, $K_{sv}$ = dynamic quenching constant, [Q] = concentration of quencher respectively, $\tau_0$ = fluorescence lifetime of tryptophan in HSA at around $10^{-8}$ s.

Fluorescence intensities were corrected for the inner-filter effect of examined compounds according to **Equation S2**:

$$F_c = F_o 10^{\frac{(A_{em} + A_{ex})}{2}} \quad \textbf{(Equation S2)}$$

where $F_0$ = measured fluorescence intensity, $F_c$ = corrected fluorescence intensity, $A_{ex}$ = absorbance of a quencher at excitation, and $A_{em}$ = absorbance of a quencher at peak emission wavelength (340 nm).

The binding constant, $K_a$, and the number of binding sites, $n$, were calculated using **Equation S3**:[1]

$$log\frac{Fo - F}{F} = -n\, log\frac{1}{[L] - [P]\frac{Fo - F}{Fo}} + n\log K_a \quad \textbf{(Equation S3)}$$

where [L] and [P] are the total concentration of complex (**1–6**) and protein (HSA), respectively.

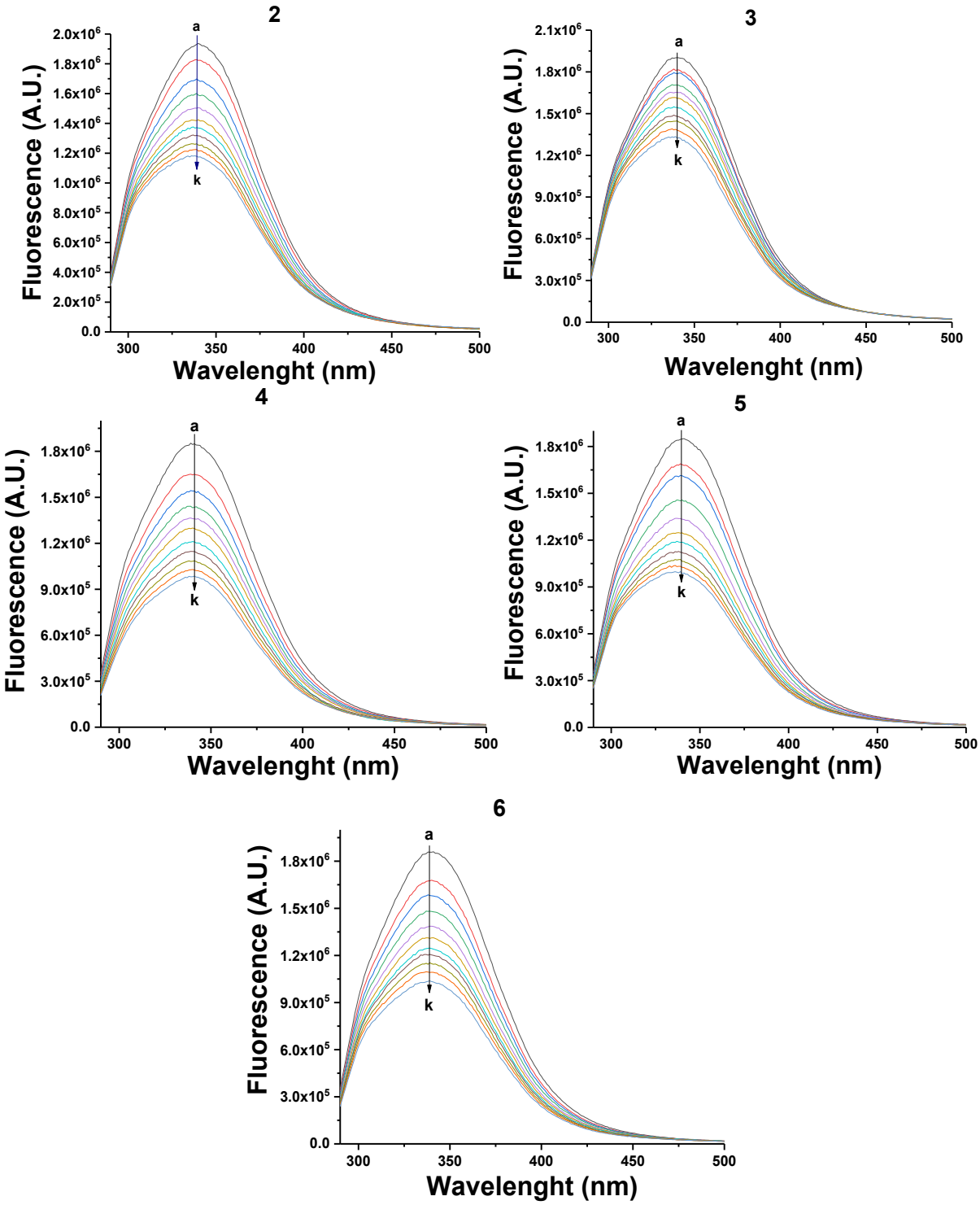


**Figure S1.** Fluorescence titration spectra of HSA (1 μM) at different concentrations of complexes **1**–**6** (0.01 M phosphate buffer solution, pH=7.4, at 25 °C). Arrow shows changes in fluorescence intensity upon increasing concentration of complexes **1**–**6** (0–10 μM).

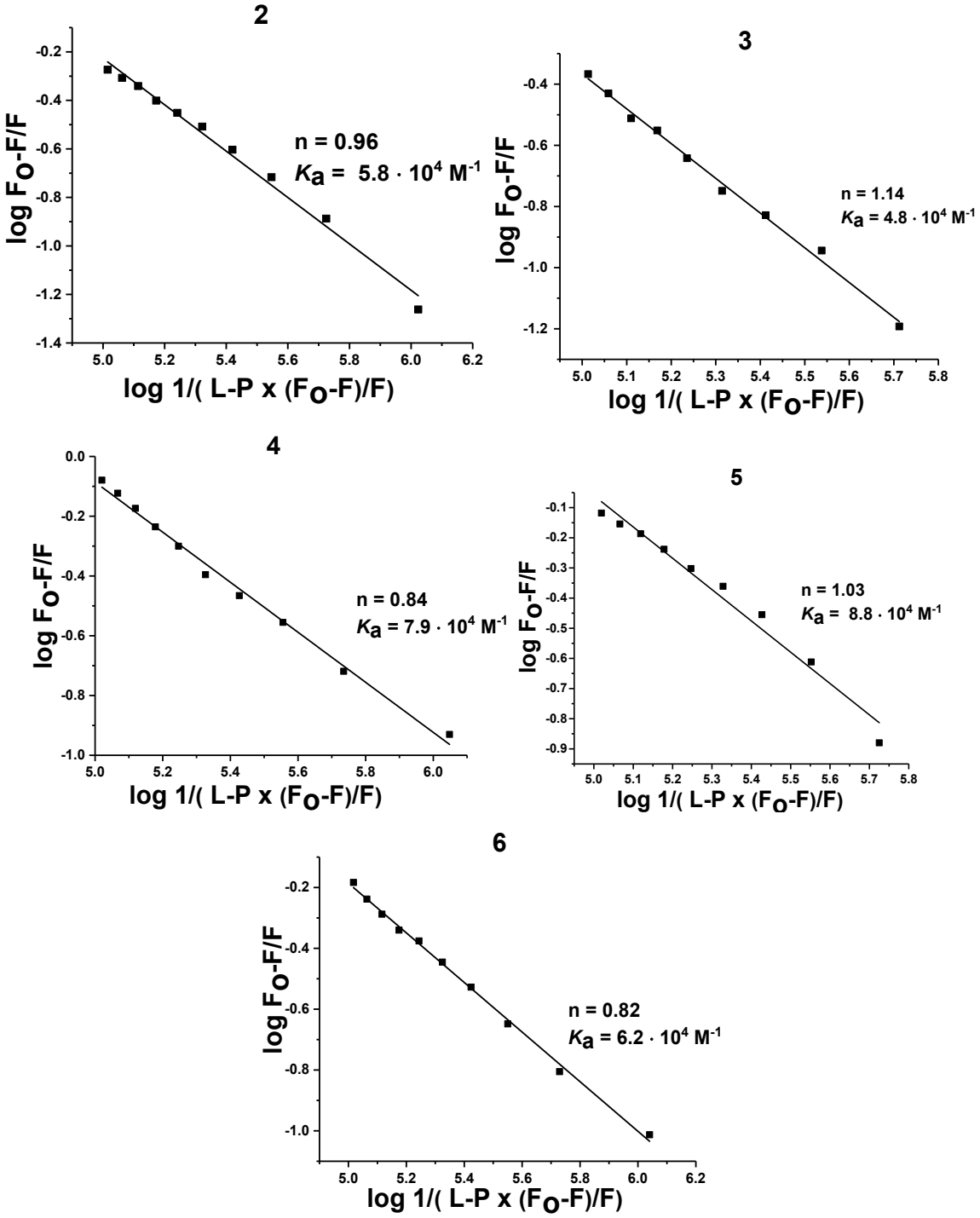


**Figure S2.** Stern-Volmer plots of the complexes 1–6 binding constant with HSA at 25 °C.

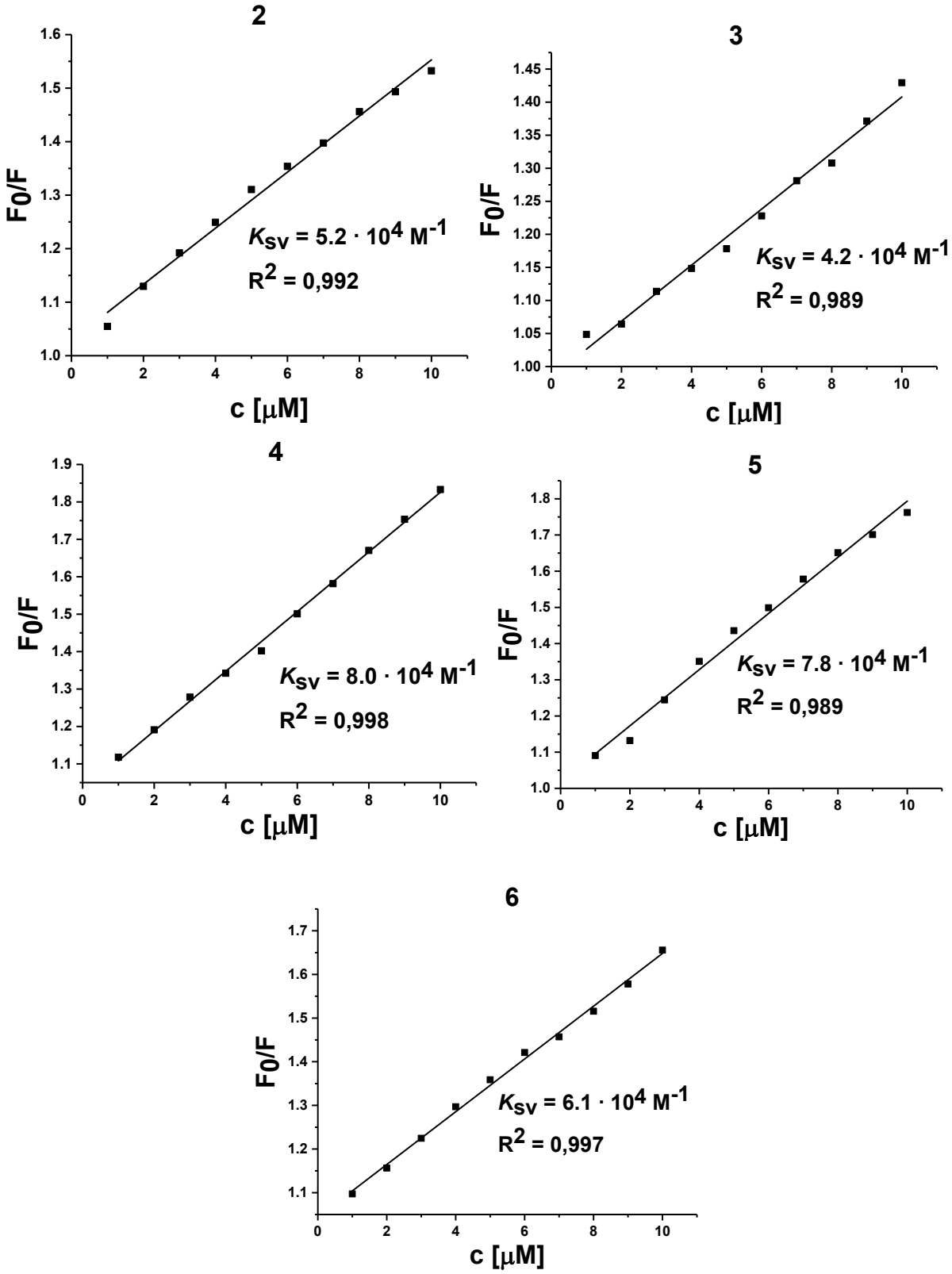


**Figure S3.** Stern-Volmer plots for the fluorescence quenching of the complexes **1**–**6** with HSA at 25 °C.

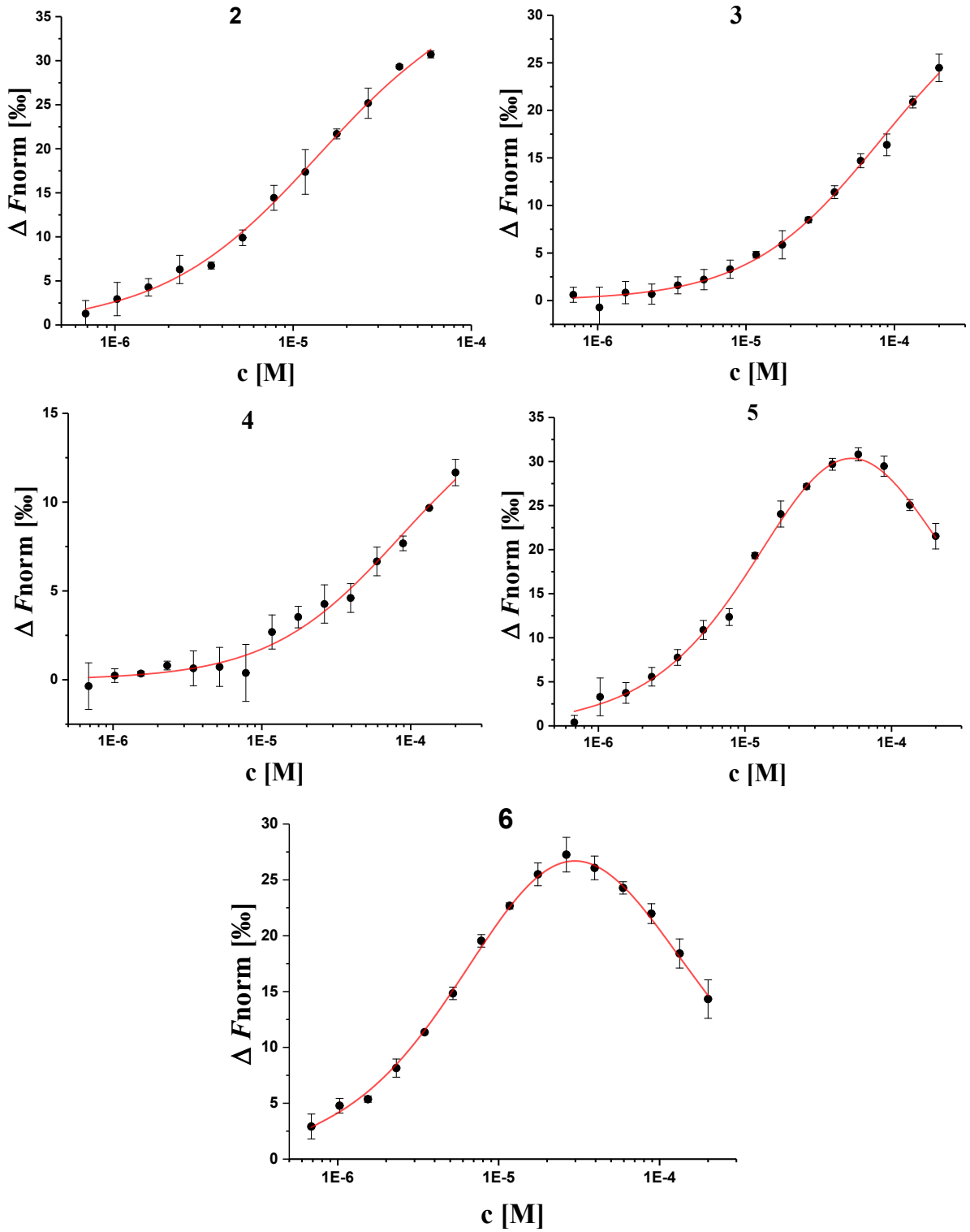


**Figure S4.** The microscale thermophoresis signal used determines the binding constant ($K_a$). The concentration of the labeled HSA was kept constant (20 nM) while the concentrations of the copper complex compounds (**3**–**6**) varied between $6.85 \cdot 10^{-7}$ M and $2 \cdot 10^{-4}$ M. Due to poor solubility, the concentrations of complex **2** varied between $6.85 \cdot 10^{-7}$ M and $5.93 \cdot 10^{-5}$ M.

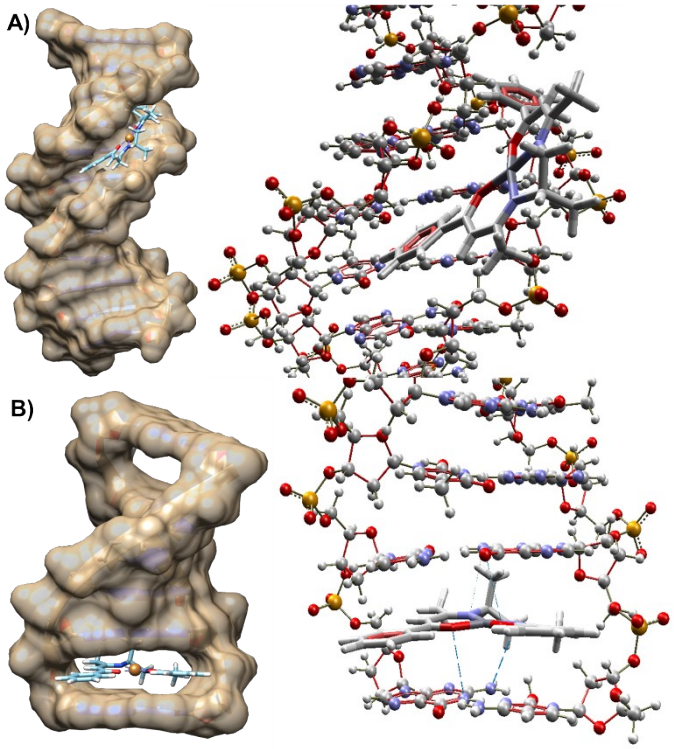


**Figure S5.** Computational docking model illustrating interactions between complex **2** and DNA: **A)** with the canonical gap (1BNA); **B)** with the intercalation gap (1Z3F) (dotted lines display a possibility of forming hydrogen bonds).

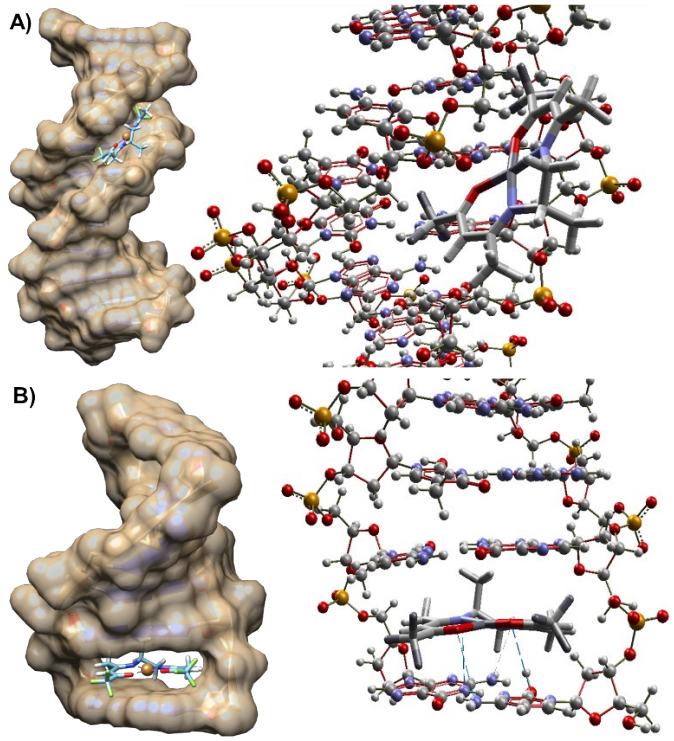


**Figure S6.** Computational docking model illustrating interactions between complex **3** and DNA: **A)** with the canonical gap (1BNA); **B)** with the intercalation gap (1Z3F) (dotted lines display a possibility of forming hydrogen bonds).

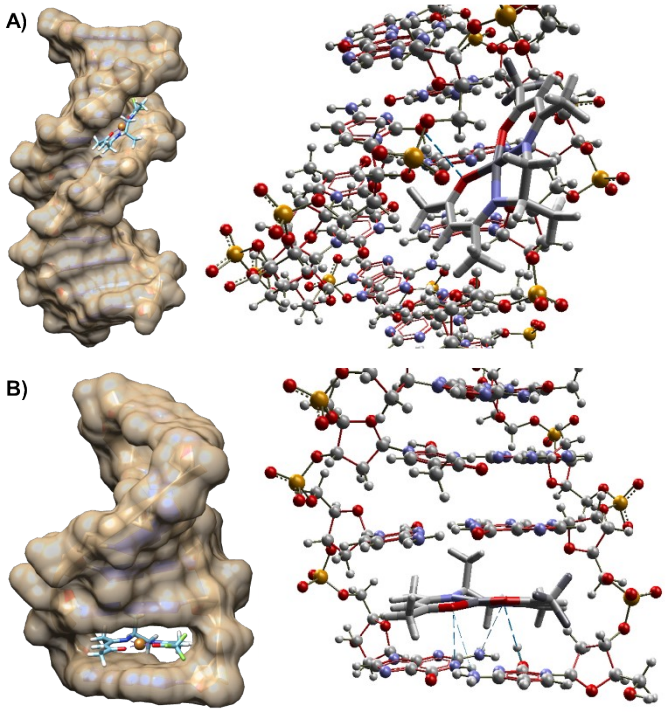


**Figure S7.** Computational docking model illustrating interactions between complex **4** and DNA: **A)** with the canonical gap (1BNA); **B)** with the intercalation gap (1Z3F) (dotted lines display a possibility of forming hydrogen bonds).

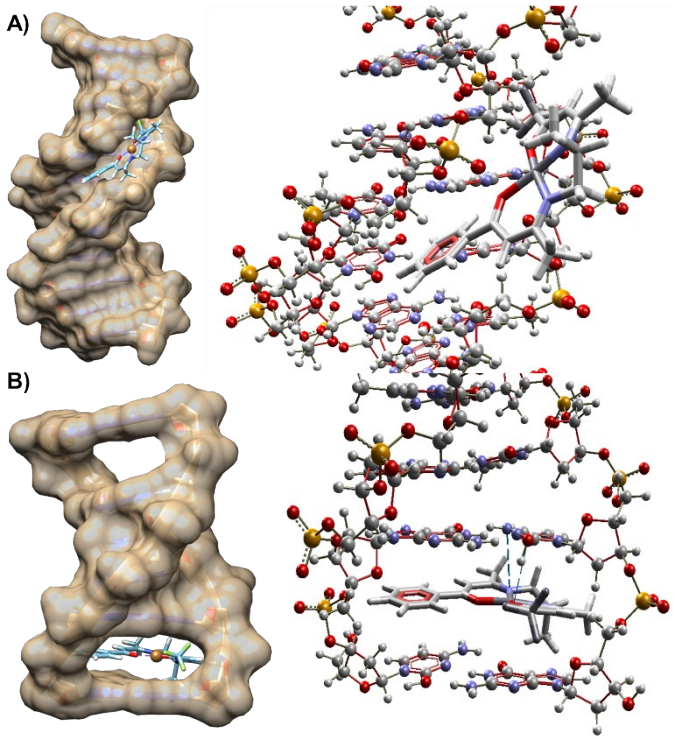


**Figure S8.** Computational docking model illustrating interactions between complex **5** and DNA: **A)** with the canonical gap (1BNA); **B)** with the intercalation gap (1Z3F) (dotted lines display a possibility of forming hydrogen bonds).

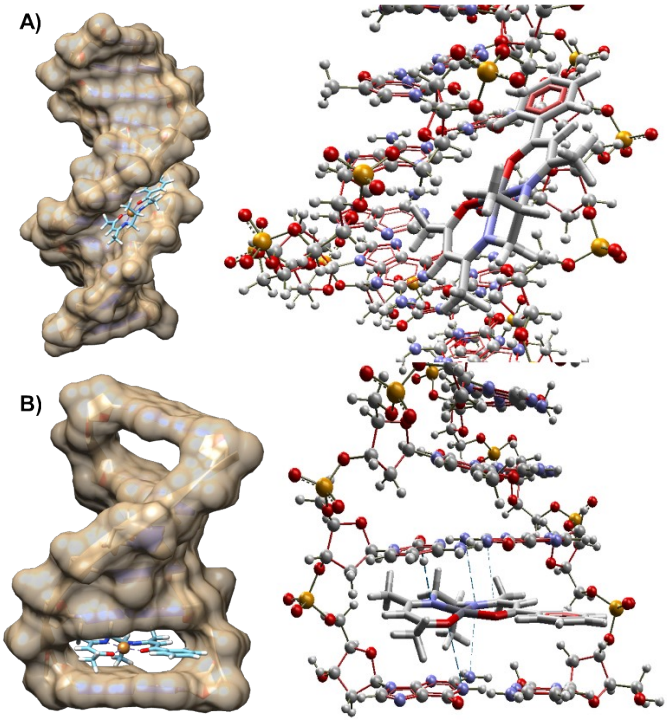


**Figure S9.** Computational docking model illustrating interactions between complex **6** and DNA: **A)** with the canonical gap (1BNA); **B)** with the intercalation gap (1Z3F) (dotted lines display a possibility of forming hydrogen bonds).

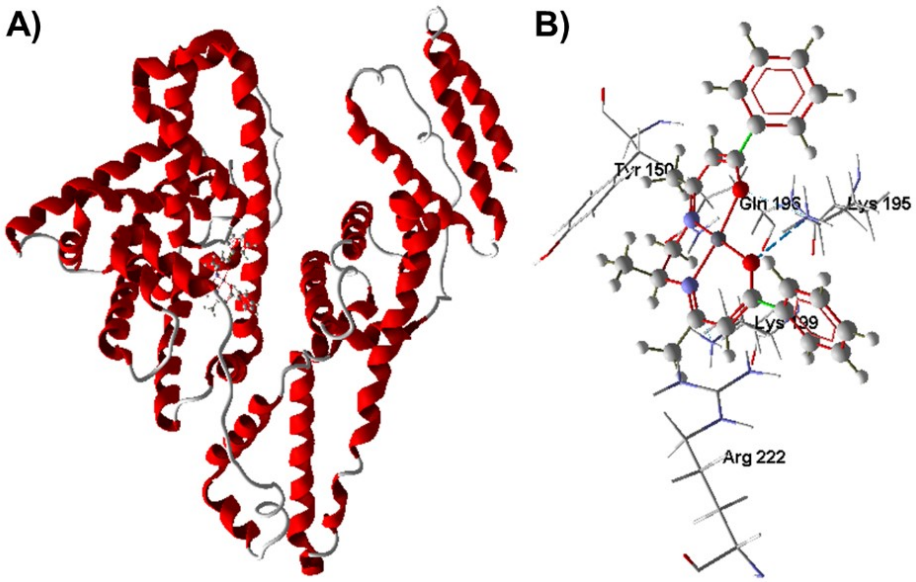


**Figure S10.** Best poses with HSA docked into a subdomain IIA for complex **2** according to Hbond values: A) molecular docking results illustrated regarding the HSA protein's backbone; B) binding site of investigated complexes on HSA proteins and selected amino acid residues (selected by applying an energy threshold of 0.625) represented by stick models (hydrogen bonds are shown as blue dotted lines).

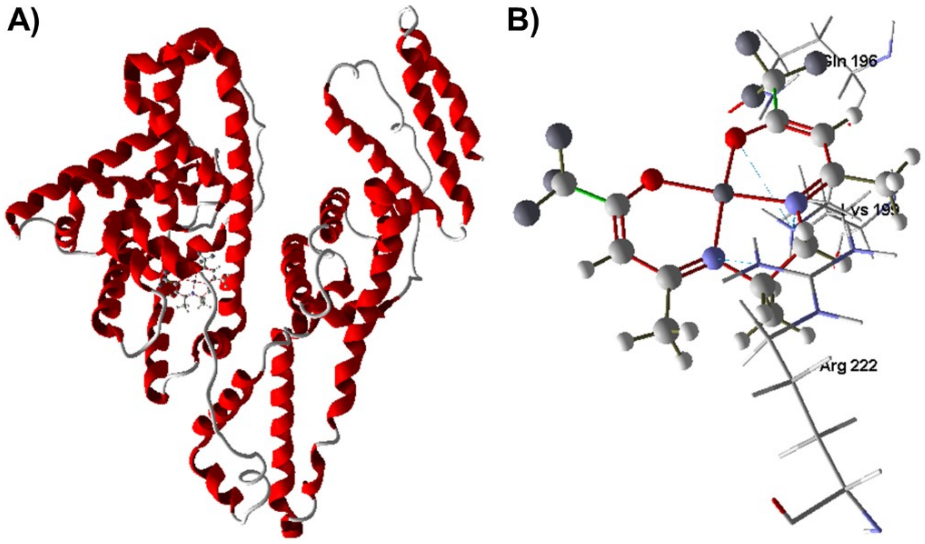


**Figure S11.** Best poses with HSA docked into a subdomain IIA for complex **3** according to Hbond values: A) molecular docking results illustrated regarding the HSA protein's backbone; B) binding site of investigated complexes on HSA proteins and selected amino acid residues (selected by applying an energy threshold of 0.625) represented by stick models (hydrogen bonds are shown as blue dotted lines).

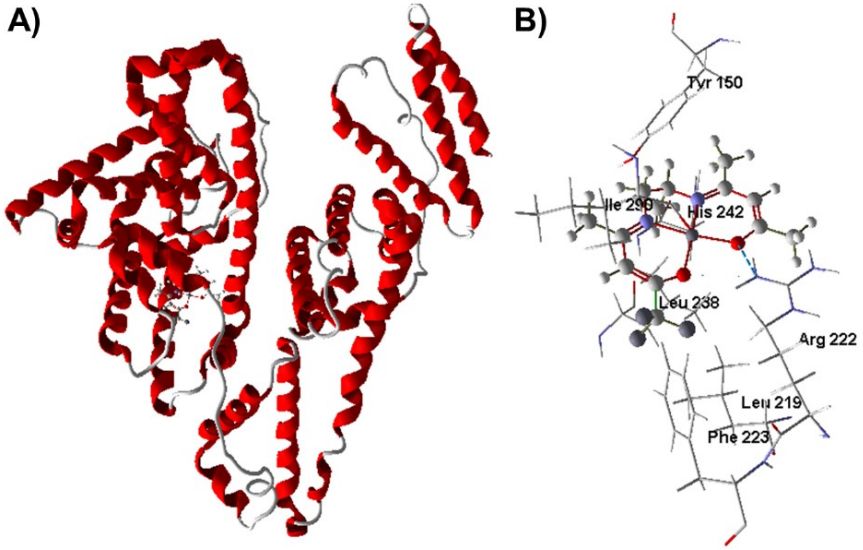


**Figure S12.** Best poses with HSA docked into a subdomain IIA for complex **4** according to Hbond values: A) molecular docking results illustrated regarding the HSA protein's backbone; B) binding site of investigated complexes on HSA proteins and selected amino acid residues (selected by applying an energy threshold of 0.625) represented by stick models (hydrogen bonds are shown as blue dotted lines).

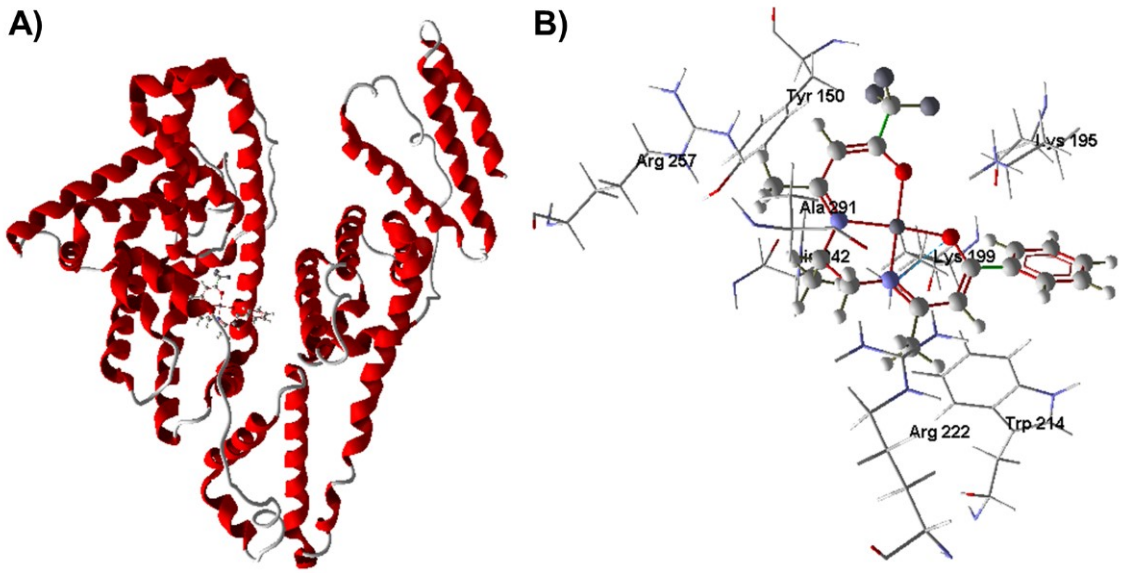


**Figure S13.** Best poses with HSA docked into a subdomain IIA for complex **5** according to Hbond values: A) molecular docking results illustrated regarding the HSA protein's backbone; B) binding site of investigated complexes on HSA proteins and selected amino acid residues (selected by applying an energy threshold of 0.625) represented by stick models (hydrogen bonds are shown as blue dotted lines).

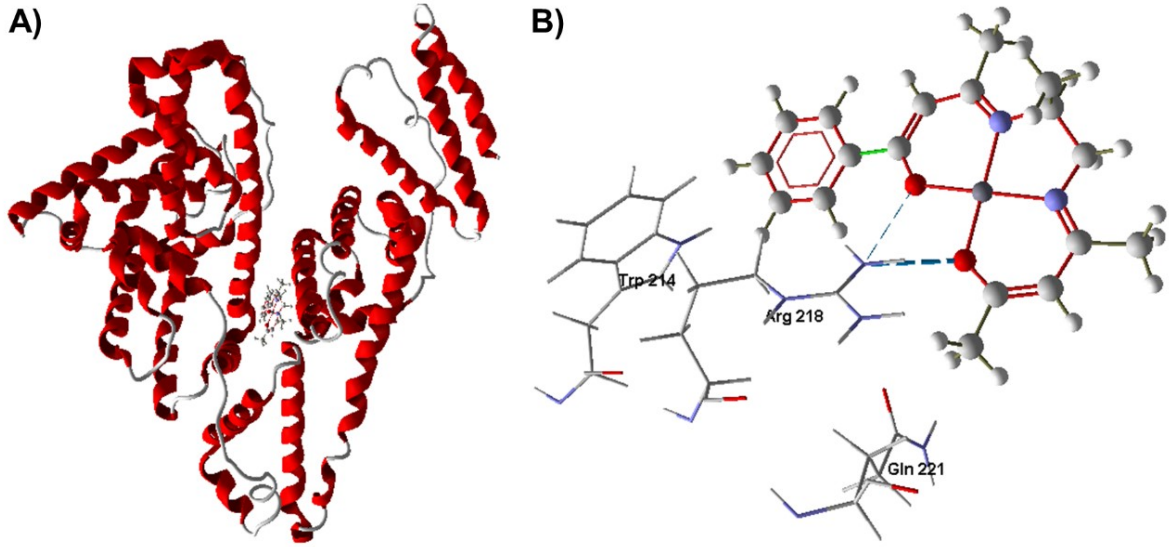


**Figure S14.** Best poses with HSA docked into a subdomain IIA for complex **6** according to Hbond values: A) molecular docking results illustrated regarding the HSA protein's backbone; B) binding site of investigated complexes on HSA proteins and selected amino acid residues (selected by applying an energy threshold of 0.625) represented by stick models (hydrogen bonds are shown as blue dotted lines).

## Reference

1 S. Bi, L. Dinga, Y. Tiana, D. Songa, X. Zhou, X. Liua and H. Zhanga, *J. Mol. Struct.*, 2004, **703**, 37–45.